Molecular Theory of Bending Elasticity and Branching of Cylindrical Micelles

Sylvio May, Yardena Bohbot, and Avinoam Ben-Shaul*

Department of Physical Chemistry and the Fritz Haber Research Center, The Hebrew University of Jerusalem, Jerusalem 91904, Israel

Received: April 16, 1997; In Final Form: June 12, 1997[⊗]

Two structural−thermodynamic characteristics of cylindrical, wormlike micelles in dilute solution are studied using a molecular-level model: (a) the bending elasticity of the micelles and (b) their tendency to form intermicellar junctions (branches). The internal (free) energy of the micelles, before and after a bending deformation and junction formation, are calculated using mean field theories for the free energies of the molecules constituting these structures. The molecular free energies, which depend on the local packing geometries, include the contributions of head group repulsion forces, the hydrocarbon−water interfacial energy, and the chain conformational free energy. We find that when only the head group and surface contributions to the packing energy are taken into account, the one-dimensional bending constant of the micelles is negligibly small. When the chain contribution is included, and when reasonable molecular packing parameters are used, we find that the persistence length, which is proportional to the bending rigidity, is typically a few tens of nanometers. The free energy change associated with the formation of a trijoint intermicellar junction upon the "fusion" of one micellar end cap with the cylindrical body of another micelle is found to be small but positive; about 10 k_BT at room temperature. This conclusion does not refute the possibility that intermicellar junctions are metastable transients or that their formation may be favored entropically, due either to conformational degeneracy or excluded volume interactions between micelles. Our conclusions apply to aqueous solutions containing one, single-tail, surfactant species.

1. Introduction

Many aqueous surfactant solutions exhibit the formation of long and flexible linear micelles, commonly referred to as "wormlike" or "threadlike".[1−7] In most cases these micelles consist of ionic amphiphiles and appear at high excess salt concentration. The major effect of the added salt is to screen the electrostatic repulsion between the charged head groups of the amphiphiles, thus lowering the optimal area per head group at the hydrocarbon−water interface of the micelle. This, in turn, implies an increase in the end cap energy, measuring the difference between the packing free energy in the highly curved (approximately hemispherical) end caps of the micelle and its (moderately curved) cylindrical body.[8−12] Consequently, the average micellar length, $\langle L \rangle$, which increases exponentially with the end cap energy, can be dramatically enhanced, leading to the formation of "giant" micelles.[1] Another relevant length scale in these systems is the *persistence length*, ξ, measuring the range (the "coherence length") of angular correlations along the micellar axis.[1,13,14]

As in the case of polymers, the persistence length is proportional to κ, the one-dimensional (1D) bending modulus of the micelle ($\xi = \kappa/k_BT$) which determines the free energy cost of linear curvature deformations (k_B is Boltzmann's constant and T the absolute temperature). Thus, ξ, like the end cap energy, is an intrinsic property of the micelle, governed by the dependence of the molecular packing free energy on the local aggregation geometry[8−12] (interfacial curvature and area per head group). When $\xi \ll \langle L \rangle$ the micelles are highly tortuous, i.e., wormlike. When $\xi \sim \langle L \rangle$, they are semiflexible,[15] and when $\xi \gg \langle L \rangle$, the micelles can be treated as rigid rods.

Micellar flexibility plays a crucial role in both the thermodynamic (phase) and dynamic (rheological) behaviors of self-assembling surfactant solutions. For instance, the isotropic−nematic transition in solutions of rigid (rodlike) micelles is accompanied by a dramatic increase in the average micellar size in the nematic phase.[11,15−18] Increased micellar flexibility greatly diminishes this coupling between orientational order and micellar growth.

Wormlike micelles are often referred to as "living polymers"[4−6] because, being relatively "soft" aggregates, their size distribution, unlike that of normal polymers, is constantly equilibrated according to the ambient conditions, such as the temperature, the total surfactant concentration, or the amount of added salt. This unique property is sometimes reflected in an unusual rheological behavior. For instance, in several ionic surfactant solutions, it was found that upon increasing the salt concentration and hence the average micellar length, the zero shear viscosity does not increase monotonically but, rather, shows a maximum as a function of the added salt concentration.[6,19,20] As in ordinary polymer solutions, the initial increase in viscosity may be attributed to entanglement effects. However, micellar (living) polymers, albeit at a certain free energy cost, can cross each other or even cross-link to form branched[19,26] micelles. Micellar crossings and the formation of (fluidlike and hence mobile) intermicellar junctions may explain the decreasing viscosity at high salt concentrations.[5,6,19−22]

It has been suggested that at high surfactant concentrations the intermicellar junctions proliferate to the extent that a cross-linked network of cylindrical micelles is formed, either spanning the whole system or separating as a densely connected phase coexisting with a very dilute phase of small micelles.[5,6,19−23] It is not obvious however whether this network (gel) formation is driven by energetic or entropic factors or perhaps by both. Recent cryotransmission electron microscopy experiments have clearly demonstrated the formation of branched threadlike micelles in several surfactant systems.[25,26] But, again, it is not fully clear whether these are truly equilibrium structures or perhaps metastable intermediates resulting from shear stresses in the course of sample preparation.

[⊗] Abstract published in *Advance ACS Abstracts,* October 1, 1997.

S1089-5647(97)01328-X CCC: $14.00

There has been enormous interest in the elastic properties of lipid monolayers and bilayers. This has motivated the formulation of both phenomenological and molecular level theories for the curvature and stretching elasticity moduli of these systems.[27−29] Surprisingly, as far as we are aware of, despite the great interest in the elastic properties of cylindrical micelles, no microscopic model has so far been suggested for estimating their 1D bending modulus κ. One of our two main goals in the present paper is to present such a model and to provide numerical estimates for this bending modulus.

Our second, related goal is to present a molecular-level model and numerical estimates for the free energy change associated with the formation of an intermicellar junction. A very simple model of this structure, based on elementary packing (surface/volume) considerations, was suggested about a decade ago by Porte *et al*.[30] The model presented in this paper is considerably more detailed, taking into account all of the relevant (head group, surface, and chain) contributions to the free energy of this rather complex (mostly saddlelike) amphiphile packing geometry.

Spherical and (straight) cylindrical micelles or planar bilayers are uniform aggregation geometries, in the sense that all the constituent amphiphiles are (on average) subjected to the same packing constraints. On the other hand, intermicellar junctions or bent cylindrical micelles are nonuniform packing geometries, involving regions of different curvatures and surface volume ratios. The volumes and hence the number of molecules in these regions are adjusted so as to minimize the total free energy of the composite nonuniform structure. This presents some difficulties in the free energy calculations, especially for the case of intermicellar junctions. Our way of treating this problem is discussed in section 4. Beforehand, in section 2, we outline the basic assumptions and structural models used in our free energy calculations, and in section 3 we present our model for calculating the bending free energy of cylindrical micelles.

2. Free Energy

Consider a micellar aggregate, or a section thereof, composed of N amphiphilic molecules. $\sigma(s)$ denotes the local surface density of head groups around point s of the hydrocarbon−water interface (hereafter "the interface") and $f(s)$ the local free energy per molecule at this point. In a nonuniform structure, such as an intermicellar junction or a bent cylindrical micelle, both the head group density (which depends on the local surface−volume ratio) and the free energy per molecule are functions of s. The total free energy of the aggregate is

$$F = \int \mathrm{d}s\, \sigma(s)\, f(s) \tag{1}$$

Similarly, the total (hydrophobic) volume of the aggregate is

$$V = \nu \int \mathrm{d}s\, \sigma(s) = N\nu \tag{2}$$

where ν is the volume of the amphiphile hydrocarbon tail, as measured in the liquid state of the corresponding alkane. As usual, we assume here that the density of the hydrocarbon chain segments within the hydrophobic core of the aggregate is uniform and liquid like.[8−12]

Another common assumption to be employed throughout this paper is that, at any local packing environment (s), the free energy per molecule can be expressed as a sum[27]

$$f = f_\mathrm{h} + f_\mathrm{s} + f_\mathrm{c} \tag{3}$$

with the three terms on the right hand side representing, respectively, the average interaction (steric and/or electrostatic) energy per molecule resulting from head group repulsion, the surface energy associated with the hydrocarbon−water interface, and the chain (hydrocarbon tail) contribution to the free energy. All three terms depend on the local geometry, that is, on (i) the average cross-sectional area per molecule at the interface $a = a(s)$ and (ii) the local interfacial curvatures $c = c_1,c_2$, with $1/c_i = R_i, (i = 1, 2)$ denoting the two local radii of curvature. In most aggregation geometries, such as spherical or cylindrical micelles and lipid bilayers, the hydrocarbon tails are oriented (on average) along the normal to the interface, so that $a(s) = 1/\sigma(s)$. In more complex structures the chain "directors" may be tilted with respect to the interface, implying a slightly more complicated dependence of σ on a.

A common approximation used in phenomenological models of amphiphile self-assembly is to set $f_\mathrm{c} = g$ where g is a constant depending on the hydrocarbon tail length, but independent of the aggregation geometry.[8−11] On the basis of this "hydrocarbon droplet assumption", the packing free energy and hence the optimal aggregation geometry are governed by the balance between the two "opposing forces", namely, the head group repulsions which favor large head group areas a and the hydrocarbon−water surface energy which tends to minimize a. On the basis of this model, one can qualitatively explain why, for instance, charged single-tail surfactants generally prefer packing in curved aggregates such as spherical or cylindrical micelles, whereas double-tail phospholipids spontaneously assemble into extended bilayer sheets. However, neglecting the tail contribution to the free energy is generally insufficient for explaining certain important phenomena, such as the curvature elasticity of membranes[27] or, as we shall see below, the bending elasticity of cylindrical micelles.

The chain free energy indeed involves a constant (geometry independent) term accounting for the attractive, cohesive ("hydrophobic") energy of the aggregate. Yet, another important term arises from the tail internal free energy, whose main component is the chain conformational entropy. This entropy generally increases with increasing a and thus provides another repulsive contribution to f. The force moments of head−head and tail−tail repulsions are "concentrated" at different planes (i.e., on opposite sides of the hydrocarbon−water interface). These forces, together with the (attractive) surface-tension force, determine the equilibrium surface area and curvature of the aggregate.[27]

To calculate the chain conformational free energy, we shall employ a statistical−thermodynamic mean field theory of chain packing in amphiphilic aggregates which has previously been applied to a variety of systems and phenomena.[11, 27] This theory will be briefly outlined below. First, however, we consider the first two terms in eq 3, which, together with the assumption f_c = constant, constitute the approximation known as the "opposing forces model" (hereafter OFM). Using $f = f_\mathrm{o} = f_\mathrm{s} + f_\mathrm{h}$ to denote the OFM free energy (setting $f_\mathrm{c} = 0$), we shall represent this quantity based on the common approximation[8−10]

$$f_\mathrm{o} = \gamma a + B/a_\mathrm{h} \tag{4}$$

The first term on the right hand side of this equation is the interfacial energy, with γ denoting the effective surface tension corresponding to the hydrophobic−aqueous micellar interface. The second, head group repulsion term provides an approximate representation of steric and/or electrostatic forces, with B measuring the strength of the repulsive forces. We shall treat B as a variable controling (together with γ and chain repulsion forces) the optimal aggregation geometry. Using l_h to denote the average distance between the interface and the surface of head group repulsions, a_h is the average area per head

group at this latter surface. Thus,

$$a_h = a[1 + (c_1 + c_2)l_h + c_1c_2l_h^2] \quad (5)$$

where a, as in (4), is the head group area at the interface and c_1,c_2 are the two (local) principal curvatures, also measured at the interface; e.g., $c_1 = c_2 = 1/R$ in a spherical micelle of hydrophobic radius R, and similarly for a cylindrical micelle $c_1 = 1/R$,$c_2 = 0$.

Typically $l_h \ll l_c$ where l_c is the length of the (fully extended) hydrophobic tail, while R is generally just slightly smaller than l_c, ($R < l_c$ ensures uniforms segment density within the hydrophobic core); thus $a_h \simeq a$. Setting $a_h = a$ and minimizing (4) with respect to a, one finds the optimal area per head group according to the OFM scheme, $a_o = (B/\gamma)^{1/2}$. Ignoring again the curvature corrections implied by (5) and dropping an irrelevant additive term, one obtains the OFM free energy per molecule

$$f_o = \gamma a\left(1 - \frac{a_o}{a}\right)^2 \quad (6)$$

As is well-known, according to this model, the amphiphiles always tend to assemble into aggregates where all, or most, molecules can be packed such that $a = a_o$. When geometric packing constraints on the hydrocarbon *chains* allow more than one aggregation geometry, the molecules will preferentially form the smallest possible (mostly curved) micelles, so as to maximize (in dilute solution) the translational ("mixing") entropy of the system.[8,9] Thus, for example, when $a_o l_c/v \geq 3$, the amphiphiles aggregate in spherical micelles of radius $R = 3v/a_o$, even though they could also form cylindrical micelles of radius $R = 2v/a_o$ or planar bilayers of half-thickness $d = v/a_o$. Similarly, when $3 > a_o l_c/v \geq 2$ and $2 > a_o l_c/v \geq 1$, cylindrical micelles and planar bilayers, respectively, are the preferred aggregation geometries. Note, however, that the molecules comprising the edges of these aggregates cannot be packed with $a = a_o$. For instance, the molecules at the (supposedly) hemispherical ends of a cylindrical micelle are packed with $a = 3a_o/2$, and their excess packing free energy can be estimated using (6). This excess, end cap, energy is the thermodynamic driving force for the growth of linear micelles.

Geometric packing considerations in the above spirit can be employed to estimate the relative stability of more complex structures, e.g., the saddlelike geometry of an intermicellar junction, bent cylindrical micelles, curved bilayers, or inverted micellar aggregates. For such structures, curvature corrections of the kind implied by (5) can be important. Moreover, the chain contribution to the free energy, f_c, may be a crucial determinant of their thermodynamic stability.

The chain conformational free energy, in the mean field approximation, is given by

$$f_c = \sum_\alpha P(\alpha)\,\epsilon(\alpha) + k_B T \sum_\alpha P(\alpha) \ln P(\alpha) \quad (7)$$

with $P(\alpha)$ denoting the (normalized) probability of finding the chain in conformation α and $\epsilon(\alpha)$ is the internal energy corresponding to this conformation. (In the case of simple alkyl chains described by the rotational isomeric state model,[13] $\epsilon(\alpha)$ is determined by the trans/gauche bond sequence of the chain skeleton.) The two terms on the right hand side of the last equation represent the energetic and entropic contributions to the free energy, both depending on the local aggregation geometry through the parametric dependence of the probability distribution of chain conformations on a, c_1, and c_2.

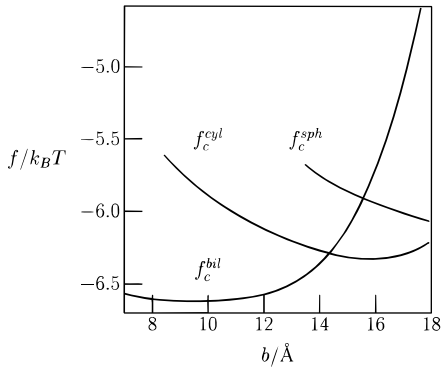

Figure 1. Chain part of the free energy per *C*14 chain in a bilayer (f_c^{bil}), cylinder (f_c^{cyl}) and sphere (f_c^{sph}) as a function of the hydrophobic radius (bilayer half-thickness or micellar radius). The upper limit $b =$ 18 Å corresponds to the fully extended hydrocarbon chain.

An explicit expression for $P(\alpha) = P(\alpha; a, c_1, c_2)$ is obtained by minimizing f_c subject to the packing constraints expressing the requirement for uniform segment density within the hydrophobic core of the aggregate. These packing constraints depend on a, c_1, and c_2. The result obtained for the conformational distribution function is[27]

$$P(\alpha) = \frac{1}{q}\exp\{-[\epsilon(\alpha) + \int dz\, \pi(z)\, \phi(\alpha,z)]/k_B T\} \quad (8)$$

where $\phi(\alpha,z)\,dz$ is the volume occupied by a chain in conformation α within a shell z, $z + dz$, parallel to the micelle interface, inside the hydrophobic core. (Thus, the z axis is along the surface normal of the aggregate; e.g., in spherical micelles z is the distance from the micellar center, etc.) The (isothermal−isobaric) partition function q ensures the normalization of $P(\alpha)$, and the function $\pi(z)$ is the lateral pressure profile. It is evaluated using the self-consistency relationships obtained by substituting (8) into the equations expressing the constraints of uniform segment density. The geometry (i.e., a, c_1, c_2) dependence of $\pi(z)$ and hence $P(\alpha)$ enters through the geometry dependence of the packing constraints. Similar expressions for $P(\alpha)$ can be derived for more complex (e.g., nonuniform) packing geometries, as well as for multicomponent aggregates.

Many complex aggregation geometries, including intermicellar junctions and flexible linear micelles, can be treated as combinations or deformations of the three "canonical" aggregation geometries, namely, spherical micelles, cylindrical micelles, and planar bilayers. It is therefore instructive to examine how the packing free energies in these three types of aggregates depend upon the relevant molecular and geometric parameters. Fixing the values of γ, l_h, and the chain length, l_c, we shall focus on the variation of f with the strength of head group repulsion, B, and the thickness, b, of the hydrophobic core (b denotes the radius of spherical and cylindrical micelles or the half-thickness of a planar bilayer). Here, as well as in the following sections, we shall use[8] $\gamma = 0.12 k_B T/\text{Å}^2 \approx 50$ dyn/cm (at room temperature), $l_h = 1$ Å, and $l_c = 18$ Å, corresponding to $-(CH_2)_{13}CH_3$ (*C*14) alkyl chains.[10] The volume of a *C*14 chain is $v \approx 405$ Å^3. We shall use this value to relate the area per molecule to the hydrophobic thickness (i.e., $a = i(v/b)$ with $i = 1$, 2, and 3 for planar bilayers, cylinders, and spheres, respectively). It should be noted, however, that neither v nor a enters directly into our chain free energy calculations; the relevant parameters there are l_c, b, and the local interfacial curvatures.

In Figure 1 we show f_c as a function of b, for the three basic geometries. In these calculations we have allowed for small roughness fluctuations (∼1 Å) of the hydrocarbon−water

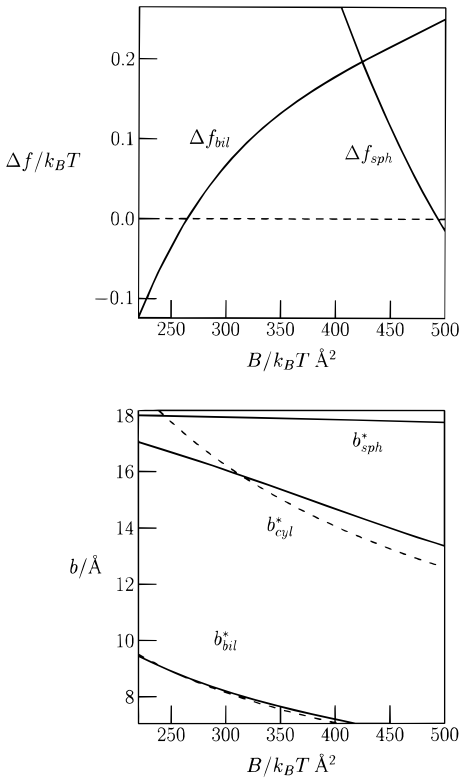

Figure 2. (a, top) Difference between the free energy per molecule in a bilayer ($\Delta f_{bil} = f_{bil} - f_{cyl}$) or a sphere ($\Delta f_{sph} = f_{sph} - f_{cyl}$) and that in a cylinder, as a function of B. (b, bottom) Corresponding aggregate thickness. The dashed lines are the optimal thicknesses according to the OFM approximation, eq 5.

interface. In all cases f_c increases steeply once b is larger than $l_c \approx 18$ Å, as this implies the creation of a "hole" in the center of the hydrophobic region. Note that the minimal value of f_c appears at different values of b in the three geometries: $b \approx$ 10, 16, and 18 Å (corresponding to $a \approx 40$, 51, and 68 Å^2) for the bilayer, cylinder, and sphere, respectively. More importantly, at variance with the hydrocarbon droplet assumption mentioned above, the free energy minima are not the same in all geometries. These small differences (a few tenths of k_BT) can be significant for determining the optimal packing geometry.

We now add the surface and head group contributions (as given by (4), with $l_h = 1$ Å) to the chain free energy and, for each value of the head group repulsion parameter B, calculate f as a function of the hydrophobic thickness b. Then, for any given B, we evaluate b^*, the value of b for which f is minimal, and identify $f = f_c(b=b^*) + f_o(b=b^*)$ as the equilibrium free energy per molecule for that particular B. Since we are mainly interested in the relative stabilities of the different packing geometries, it is convenient to choose one of these geometries, say the cylinder, as a reference: i.e., we set $f_{cyl} = 0$ and calculate $\Delta f_g = f_g - f_{cyl}$ for all B (g = sph, bil). The results obtained for Δf_g and b^* as a function of B are shown in Figure 2a,b, respectively. From Figure 2a we see that for small values of B the planar bilayer is the most stable packing geometry, for intermediate ones it is the cylinder and, as expected, spherical micelles provide the optimal aggregation geometry when head group repulsions become very strong. Moreover, as B increases, one expects an increase in the optimal area per head group, and hence a decreasing value of b^*, as confirmed by Figure 2b. The dashed curves in this figure show how $b_o = b^*$ varies with B according to the OFM scheme, i.e., when we ignore the chain conformational free energy and set $f = f_o$. The crossing points of the dashed and solid curves in this figure correspond to the minima in the chain free energies (Figure 1).

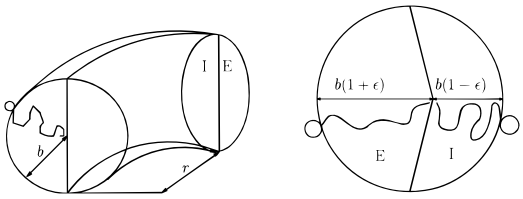

Figure 3. (Left) Toroidally bent micelle, divided into external (E) and internal (I) parts by a hypothetical surface. (Right) Cut through a bent micelle showing the extended definitions of the E and I regions. The radius of the micelle is b, and ϵ describes the asymmetry.

3. Flexibility of Cylindrical Micelles

Consider a long cylindrical micelle of radius b and suppose that a segment of length L of this micelle is uniformly bent, thus forming a section of a torus. Let r denote the radius of the torus, (measured with respect to the cylinder axis, Figure 3), and assume $r \sim L \gg b$.

The curvature deformation free energy of the cylinder, ΔF, can be expanded in a power series of the 1D curvature $c = 1/r$. By symmetry ΔF involves only even powers of c, and for small curvatures ($bc \ll 1$) can be safely approximated by the leading term,[1,13]

$$\frac{\Delta F}{L} = \frac{1}{2}\kappa c^2 \tag{9}$$

with $\kappa = (\partial^2 \Delta F/\partial c^2)_{c=0}$ defining the 1D bending modulus of the cylinder.

As mentioned already in section 1, the bending rigidity dictates the micellar persistence length, $\xi = \kappa/k_BT$, which measures the decay length of angular correlations along the micellar axis. (Alternatively, recall that $P = \exp(-\Delta F/k_BT)$ is the probability of a bending fluctuation. This probability is large, implying the loss of orientational coherence when $\Delta F/k_BT \sim 1$. From (9) it follows that this happens, for example, when the micellar axis is changing direction by forming a circular arc of length $L \sim \xi$ and radius $r = 1/c \sim \xi$).

Micellar flexibility is mainly interesting when the persistence length is significantly smaller than the average micellar length $\langle L \rangle$. In dilute solution[1,8,9,11]

$$\langle L \rangle \approx 2(\nu/\pi b^2)(X e^{\delta})^{1/2} \tag{10}$$

where X is the total mole fraction of surfactant in solution and $\delta = 2N_{cap}(f_{cap} - f_{cyl})/k_BT$ is the 1D growth parameter, or, more simply, the end cap energy. N_{cap} denotes the number of molecules in the end cap; f_{cap} and f_{cyl} are the average free energies per molecule in the end cap and the cylindrical body of the micelle, respectively. In the calculations presented in this section we shall use $B/k_BT = 300$ Å^2, implying strong preference of the amphiphiles to pack in the cylindrical body over the end cap (see Figure 2a) and hence large end cap energy ($\delta \sim 42$). For this B we also find that the optimal micellar radius for $C14$ chains is $b = b_{cyl} \approx 16$ Å (corresponding to an optimal area per head group $a = a_{cyl} = 2\nu/b_{cyl} = 51$ Å^2). The above value of δ implies extremely large $\langle L \rangle$ already at very small values of X. Note, however, that for such "giant" micelles[1] the dilute solution expression (10) is just an approximation.

Suppose that an imaginary plane, containing the cylinder principal axis, divides the micelle into two regions. Upon bending the micelle, in a plane perpendicular to the dividing plane above, these regions become the "external" (E) and "internal" (I) parts of the torus, as illustrated in Figure 3. If the length, L, of the micelle, as well as its hydrophobic radius, b, do not change in the course of bending, then its volume $V =$

$V^E + V^I$ and hence the number of chains contained in this volume are constants, independent of the torus radius r. The total interfacial area of the micelle $A = A^E + A^I$ is also conserved. Clearly, however, except in the case of the straight cylinder ($c = 1/r = 0$), the volume and surface area of the outer region are larger than those of the inner region; $V^E \geq V/2 \geq V^I$, $A^E \geq A/2 \geq A^I$. Furthermore, the surface to volume ratios of the inner and outer parts are different; in fact $A^E/V^E \geq V/A = 2/b \geq A^I/V^I$, with the equalities holding only for the straight cylinder.

In the straight cylinder the numbers of molecules in the E and I parts of the micelle are the same. Also, it can be safely assumed that, apart from small fluctuations, the chains originating at the E and I surfaces reside in the corresponding volumes. Since $V^E > V^I$, it is clear that the above mode of deformation is only possible if molecules can diffuse into the E region and out of the I region. We shall assume that such "easy" diffusion is indeed possible. Yet, there is no reason to assume that, in the bent micelle, the chains of the amphiphiles anchored to the E (I) surface are confined to the E (I) volume. If this were the case, the average areas per head group in the external and internal surfaces would necessarily be different from the optimal area per head group, ($a = 2v/b$, corresponding to the straight cylinder). This, according to the OFM scheme, would inflict a free energy penalty which could easily be avoided by letting the chains of the E surface protrude into the I volume, thus optimizing the area per molecule at both surfaces. To take this possibility into account, albeit approximately, we modify the definition of the E and I volumes by assuming that, on average, all chain ends are oriented toward one line, parallel to and at a distance ϵ from the cylindrical axis (Figure 3). We allow ϵ to depend on the torus curvature and assume, as appropriate for small deformations, that $\epsilon = \eta c$. We shall treat η as a "relaxation" parameter, to be determined by minimizing the bending free energy. We shall first consider the OFM scheme and then add the chain contribution to the deformation free energy.

For the sake of concreteness, and without loss of generality, we assume that the length of (the axis of) the toroidally bent cylinder is $L = \pi r/3$, $r = 1/c$ being the radius of the torus. The volumes of the newly defined E and I regions are given by

$$V^E = \frac{\pi b^2}{18}(3\pi r + 4b) + \frac{1}{3}\pi\epsilon b^2\left(r - \frac{\epsilon b}{3}\right)$$

$$V^I = \frac{\pi b^2}{18}(3\pi r - 4b) - \frac{1}{3}\pi\epsilon b^2\left(r - \frac{\epsilon b}{3}\right) \qquad (11)$$

The areas of the inner and outer surfaces of the torus are

$$A^E = \pi b(\pi r + 2b)/3$$

$$A^I = \pi b(\pi r - 2b)/3 \qquad (12)$$

In the OFM approximation the free energy of the torus, relative to that of the straight cylinder, is $\Delta F_o = N^E f_o^E + N^I f_o^I$, where N^E is the number of molecules in the external part of the torus and f_o^E is the free energy per molecule in this region, as given by (6), etc. Thus,

$$\frac{\Delta F_o}{\gamma} = A^E\left(1 - \frac{a_{cyl}}{a^E}\right)^2 + A^I\left(1 - \frac{a_{cyl}}{a^I}\right)^2 \qquad (13)$$

where $a_{cyl} = 2v/b$ is the area per head group in the straight cylinder, whereas $a^E = vA^E/V^E$ and $a^I = vA^I/V^I$ are the areas per head group in the external and internal parts of the torus.

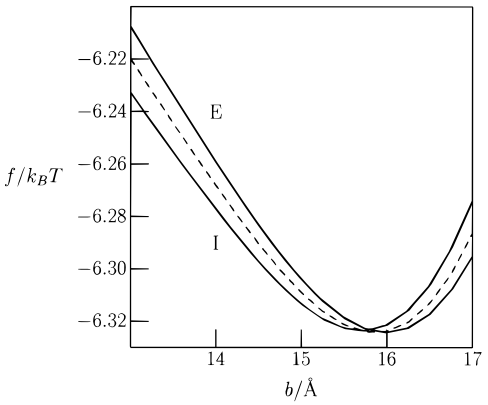

Figure 4. Average chain energy per molecule in a cylinder (broken line) as well as in the external (E) and internal (I) parts of a torus of curvature $c = 1/90$ Å^{-1} as a function of the cylinder radius b (for $\epsilon = 0$).

Using (12) and (11) to calculate a^E,a^I, substituting the resulting expressions into (13), then expanding $\Delta F_o/\gamma$ in powers of c, and comparing the quadratic term with (9), we obtain

$$\kappa_o = \frac{16b\gamma}{9\pi}(3\eta - b)^2 \qquad (14)$$

From this equation it follows immediately that for $\eta = b/3$ the bending constant vanishes identically. In other words, according to the OFM picture, at any curvature c, the hydrocarbon chains within the hydrophobic core can adjust their conformations (according to $\epsilon = bc/3$) so as to ensure that all molecules are packed at their optimal area per head group $a^E = a^I = a_{cyl}$, thus allowing the cylinder to bend at no free energy cost.

The OFM result, $\kappa = 0$, is obviously unacceptable. One minor approximation which was used in its derivation involved setting $l_h = 0$ in passing from (4) to (6), thereby assuming that the forces of head group repulsion and surface tension act at the same plane. This is a reasonable approximation in view of the fact that $l_h \ll b$. The more serious approximation we made in deriving the OFM result is, of course, the total neglect of the chain contribution to the bending free energy.

As mentioned in the previous section, the calculation of f_c requires specification of the interfacial curvatures (c_1,c_2) and the area per head group a. These parameters dictate the average distribution of chain segments within the micellar core ($\langle\phi(z)\rangle$; see (8)), which determine the $\pi(z)$ and hence $P(\alpha)$ and f_c. For simple geometries like the straight cylinder the calculation of the micelle free energy is simple, because the boundary conditions are the same for all of the chains composing the aggregate. The calculation of the aggregate free energy, though feasible, becomes considerably more tedious when the aggregate involves locally varying packing geometries, such as in the case of a torus. Although we have performed a rather detailed calculation which takes into account the variation of the local geometry in a bent micelle, we shall describe here a simpler, more approximate procedure which yields essentially the same results. (The detailed, local packing, model is applied in the free energy calculations of intermicellar junctions; see section 3 and the Appendix.)

Again we divide the micellar core into E and I parts and treat $\epsilon = \eta c$ as a variational parameter. Suppose first that $\epsilon = 0$; i.e., the E and I chains are confined to their respective semitoroidal regions. In this case, upon bending, the chains in the external and internal regions undergo splay deformations (in opposite directions). These deformations, as shown in Figure 4, involve a relatively small free energy price. Recall however

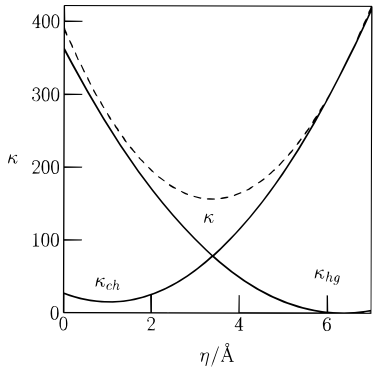

Figure 5. Bending modulus κ and its components κ_{ch} and κ_{hg} (all in units of k_BT Å) as a function of the relaxation parameter η for $B = 300\ k_BT$ Å^2. Complete relaxation is found for $\eta = 3.5$ Å.

that $\epsilon = \eta = 0$ implies a considerable free energy penalty, resulting from the fact that the head groups in both the E and I regions cannot be optimally packed; see (14).

Now, as we let ϵ increase, the head group excess energy will decrease. This implies that (on average) the E chains are further stretched and the I chains are simultaneously compressed. The extents of stretching and compressing, and hence the additional chain deformation free energy, will depend on both c and ϵ. Qualitatively, we expect that, for any c, the sum of chain and head group free energies will obtain a minimum for some finite value of ϵ, or, equivalently, the bending rigidity κ will be minimal for some finite value of η. These qualitative notions are confirmed by the calculations shown in Figure 5.

Briefly, the chain free energy calculations were done as follows. First, for every value of ϵ we determine the average chain length in the E and I (semitoroidal) regions. It can be shown that to first order in ϵ these lengths are given by

$$\bar{l}^{\mathrm{E}} = b + \frac{2b\epsilon}{\pi} = b + \frac{2b\eta}{\pi}c$$

$$\bar{l}^{\mathrm{I}} = b - \frac{2b\epsilon}{\pi} = b - \frac{2b\eta}{\pi}c \qquad (15)$$

These values are used to calculate the chain contribution to the bending free energy of two semicylinders; one of radius $\bar{l}^{\mathrm{E}}$ corresponding to the E part of the torus and the other of radius $\bar{l}^{\mathrm{I}}$ corresponding to the I part. These calculations were done for different values of ϵ (hence $\bar{l}^{\mathrm{E}}$, $\bar{l}^{\mathrm{I}}$) and different values of c. In each case chain free energies, f_c, were calculated for different head group positions along the semitorus circumference and then integrated to obtain the total micelle free energy.

Figure 5 shows the results of our calculations for the special case of *C*14 amphiphiles with head group interaction parameters $B = 300\ k_BT$ Å^2, $l_h = 1$ Å, $\gamma = 0.12\ k_BT$/Å^2. For this system, as we see in Figures 1 and 2, the optimal packing geometry is a cylindrical micelle of radius $b \approx 16$ Å. As qualitatively argued above, the chain contribution to κ increases, nearly monotonically, with η—due mainly to chain stretching and compression. On the other hand, the head group contribution (according to the OFM scheme) decreases monotonically with η, reaching zero at $\eta \simeq 6$ Å (which is somewhat larger than the value $\eta = b/3 \simeq 5.3$ Å implied by (14), because we have now used a nonvanishing l_h). The minimal value of the bending rigidity, $\xi = \kappa/k_BT \simeq 160$ Å, is found for $\eta \simeq 3.5$.

The value we found for ξ agrees, roughly, with the values found for the persistence length in some semidilute solutions of ionic wormlike micelles at high salt concentrations.[1] Had we chosen higher values for l_h, we would obtain larger values for ξ. Recall, however, that our molecular model, especially the representation of head group repulsions, was rather approximate. Our main goal was to get a reasonable estimate of the 1D bending rigidity.

The results above could also be obtained using a simple model from which an expression for κ can be derived in a closed form. From Figure 2 we note that both the head group and the chain contributions to the molecular free energy in a cylindrical micelle are minimal for approximately the same value of b ($b \simeq 16$ Å). Thus, in addition to the quadratic form (6) for the head group free energy, we can use a quadratic approximation for f_c around its minimum. Now recall that in our calculation of the chain contribution to the bending energy we have treated the E and I parts of the torus as semitori of radii $\bar{l}^{\mathrm{E}}$, $\bar{l}^{\mathrm{I}}$. Thus, the free energy per molecule in the E part for instance can be expressed as

$$\frac{f^{\mathrm{E}}}{\gamma} = a^{\mathrm{E}}\left(1 - \frac{a_{\mathrm{cyl}}}{a^{\mathrm{E}}}\right)^2 + \tau a_{\mathrm{cyl}}\left(\frac{\bar{l}^{\mathrm{E}} - b}{b}\right)^2 \qquad (16)$$

with $\bar{l}^{\mathrm{E}}$ given by eq 15 and with τ evaluated from the curvature of the chain free energy in a cylinder. (From Figure 1, $\tau \simeq 1$.) A similar expression can be written for the free energy per molecule in the inner part of the torus. The total deformation energy is given by $\Delta F/\nu = V^{\mathrm{E}}f^{\mathrm{E}} + V^{\mathrm{I}}f^{\mathrm{I}}$, where all factors depend on the curvature c. Expanding ΔF in powers of c we get κ from the second order term. The result is

$$\kappa = \frac{16b\gamma}{9\pi}[b^2 - 6b\eta + 9\eta^2(1+\tau)] \qquad (17)$$

Minimization with respect to η gives

$$\eta = \frac{b}{3(1+\tau)} \qquad (18)$$

$$\kappa = \frac{16b^3\gamma\tau}{9\pi(1+\tau)} \qquad (19)$$

For $\tau = 1$, $b = 16$ Å, and $\gamma = 0.12\ k_BT$/Å^2 we obtain $\eta = 2.7$ Å and $\kappa = 140\ k_BT$ Å, in close agreement with the detailed numerical calculation.

We conclude this section with two comments. The first comment concerns the assumption that the bent cylinder forms a section of a perfect torus, so that its cross-section is a circle. This assumption is closely related to another assumption we made, namely, that within this circular cross-section all chain ends are pointing toward one point. Subject to this assumption it can be shown by (somewhat lengthy) functional variation that the optimal shape of the bent cylinder is, indeed, a torus. A simpler, qualitative explanation of this result can easily be given for the limiting (but quite common) case where the optimal radius of the straight cylinder, b, is equal to the length of the fully stretched hydrocarbon tail, l_c. In this case, if the length, L, of the cylinder does not change in the course of bending (as appropriate for a pure bending deformation), the cross-section of the bent cylinder must remain circular, since only this shape allows all chain ends to meet at one point (which must be at the center of the circle, i.e., $\epsilon = 0$ in Figure 3.). It is of course possible that the cross-section of the bent cylinder will not be circular but, e.g., elliptical, in which case the chain ends will not meet at one point. We have considered several geometries of this kind, all leading to larger values of κ than those we found for the torus. In conclusion, if a more favorable geometry than the torus is available for the bent cylinder, then our estimate of κ should be regarded as an upper bound.

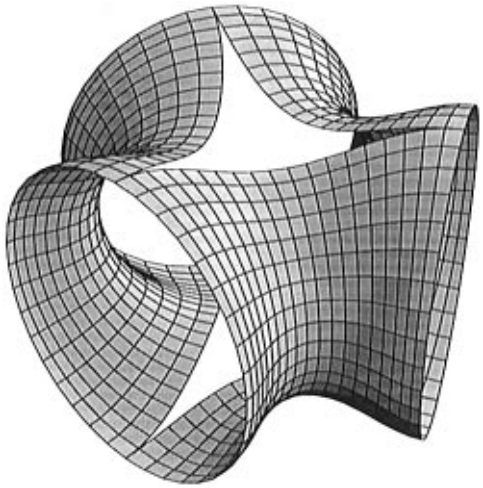

Figure 6. Surface of the Y-junction model used in the calculations. For this particular case $r/b = 2$ and $\alpha = 0.13$ (see text). The middle part (not shown) is treated as a (pinched) bilayer piece.

Finally it should be mentioned that a crude estimate of the 1D bending rigidity κ can be obtained using the more common 2D bending rigidity of surfactant layers, K, as follows. The bending energy of a surfactant monolayer of area A is given by the familiar (Helfrich) expression[31]

$$\frac{\Delta F}{A} = \frac{1}{2}K(c_1 + c_2 - c_0)^2 + \bar{K}c_1c_2 \qquad (20)$$

with K and $\bar{K}$ denoting the splay and saddle-splay bending constants, respectively, and c_0 being the spontaneous curvature. Recall that the bending free energy is minimal when $c_1 = c_2 = c_{eq} = c_0K/(2K + \bar{K})$. Suppose now that the cylinder is composed of two semicylinders, E and I, as in Figure 3. The E semicylinder can be regarded as a monolayer with one (very) high principal curvature $c_1 \approx 1/b$ and one moderate curvature $c_2 \approx 1/r$, where r is the radius of the torus. (Actually, both curvatures should be measured with respect to the neutral surface of the monolayer which typically lies somewhere inside the hydrophobic core, implying $c_1 > 1/b$. Note also that $c_2 = 1/r$ is only approximately valid.) Similarly, for the I semicylinder $c_1 \approx 1/b$ and $c_2 \approx -1/r$. Using eq 20 for the E and I semicylinders and adding their contributions to the bending energy, we find $\Delta F = AK/r^2 = LdK/r^2$, where L is the length of the bent cylinder and $d \sim$ b is the width of the semicylindrical monolayers ($d = \pi b$ if the neutral surface is exactly at the interface). Hence, the 1D and 2D bending constants are related by $\kappa = 2dK \sim bK$, a result which could also be guessed by dimensional analysis. Typically, for lipid bilayers, $K \sim 10\ k_BT$, and, hence, with $b = 15$ Å, we find that κ is of the order of several hundreds of k_BT Å, consistent with our findings.

Of course, the above expression for ΔF is only valid for small curvature deformations (c_1 and c_2 close to c_{eq}). Hence, using the (near planar) monolayer value for K to estimate κ is certainly a far reaching approximation. Yet it is interesting to note that this crude approximation provides a reasonable order of magnitude estimate for κ.

4. Intermicellar Junctions

In Figure 6 we show our model for a 3-fold ("Y-like") intermicellar junction. The three cylindrical micelles join each other through matching semitoroidal sections, and the middle of the structure is completed by a trianangular bilayer "patch". The local geometry of the semitoroidal regions is saddlelike. The bilayer region is "pinched", thus enabling the amphiphiles to pack at a larger area per head group, closer to that in the cylindrical branches. The exact parametrization of the junction surface is given in the Appendix. The extent of the pinching is taken into account through a parameter α. When $\alpha = 0$ the bilayer thickness exactly matches the diameter $2b$ of the semitoroidal regions; b is also the radius of the cylindrical micelles forming the junction. When $\alpha > 0$ the bilayer thickness decreases continuously toward the center of the junction, reaching a minimum value of $2b(1 - 2\alpha)$ in the middle of each toroidal section. Another important geometrical characteristic of the junction is the radius of the (negatively bent) semitori r. Both r and α will be treated as variational parameters, to be determined by minimization of the total free energy of the junction.

The packing geometry of the amphiphiles constituting the junction is not uniform, involving locally varying surface to volume ratios at different points of the structure. Even after optimization of the junction size and shape with respect to r and α, it is not possible to pack all amphiphiles with the same area per head group and (certainly) not at the same local curvatures of the interface. So, obviously, if the cylindrical micellar geometry provides the optimal packing conditions, there is no energetic incentive for micellar branching. It is however possible that the "fusion reaction" where a junction is formed by the fusion of an end cap of one micelle with the cylindrical body of another is energetically favorable. Then one might expect the appearance of micellar junctions at concentrated micellar solutions. It is also possible that the saddlelike geometry which constitutes a considerable portion of the aggregate provides a convenient packing geometry. If the saddle energy is substantially lower than that of the cylinder, one expects the formation of inverted cubic phases already at low amphiphile concentrations, as indeed observed in some lipid solutions. If the energies of the cylinder and the saddle are comparable (i.e., within several k_BT's), one can expect junction formation already in dilute and semidilute micellar solutions, at least as metastable structures. The free energy calculations presented here are intended to help answer these questions.

Since junctions were experimentally observed in solutions of wormlike micelles, we assume that the preferred aggregation geometry of the amphiphiles, at least in dilute solution, is cylindrical. The fact that, on average, the surface to volume ratio of the junction (in both its middle and saddle regions) is similar to that of a planar bilayer suggests that the cylinder stability relative to the bilayer is only marginal; in our Figure 2 this corresponds to $B \sim 300\ k_BT$ Å^2 for $C14$ chains. This also implies a large end cap energy and hence long wormlike micelles. These considerations will guide our choice of parameters in the numerical examples.

Since not all molecules in the junction can pack at their optimal area per head group, the free energy of junction formation must be finite, even according to the OFM approximation which totally ignores the chain contributions. Thus, here, as opposed to the case of the bent cylinder both the head groups and the chains will contribute to the packing free energy. To somewhat simplify the geometrical parametrization of the junction, we shall treat the middle (pinched bilayer) section as composed of two regions (Figure 7): a central, triangular piece of a flat bilayer and three slanted bilayer regions joining the flat central region with the semitoroidal edges. We shall designate the toroidal, slanted, and middle bilayer regions as t, s, and b, respectively.

The free energy of the junction is calculated as the sum of the free energies of the t, s, and b regions; their absolute and relative contributions depend on both r and α. For each region

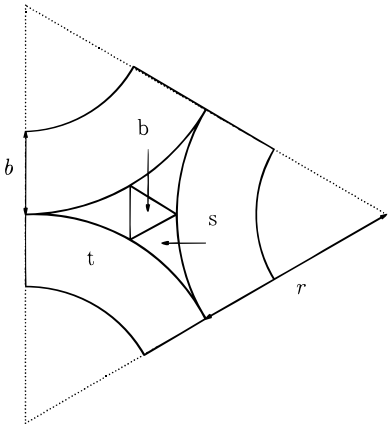

Figure 7. Top view on the bilayer part of a junction (drawn in solid lines), showing the toroidal (t) edges of the junction and the slanted (s) and flat (b) bilayer regions in its middle part.

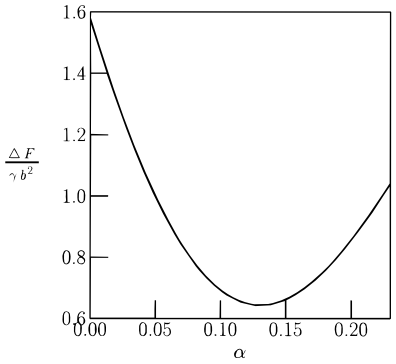

Figure 8. Optimal dimensionless energy $\Delta F/(\gamma b^2)$ of a junction as a function of the relaxation parameter, for $b = 16$ Å ($\gamma b^2 = 23.5\ k_BT$).

the free energy is given as an integral over local free energies per molecule, according to eq 1. Both the head group and the chain contributions are taken into account. The head group terms are calculated using (4), with the appropriate local head group area $a = a(s)$. We consider several values of B, always with $\gamma = 0.12\ k_BT/$Å^2 and $l_h = 1$ Å. The calculation of the ($C14$) chain free energy in the b region is straightforward. In the s region it is calculated as the value corresponding to the average bilayer thickness in this region. A more complicated procedure is needed for calculating f_c in the semitoroidal sections (see Appendix). Here, when $\alpha > 0$, the inner radius of the semitori ($b(\phi)$) is not constant, passing through a minimum between every two cylindrical branches. The chain free energy is calculated, for every r and α, as a function of $b(\phi)$, and then integrated to yield the total semitorus energy.

In Figure 8 we show the total junction free energy ΔF, after minimization with respect to r, as a function of α; calculated according to the (locally applied) OFM approximation; i.e., the chain contribution is not included in this calculation. The energy is calculated relative to the packing energy in a cylindrical micelle of radius $b = 16$ Å, corresponding to a head group repulsion strength $B = 308\ k_BT$ Å^2. The global minimum of ΔF occurs for $\alpha \simeq 0.13$; the corresponding optimal radius is $r \simeq 24$ Å $\simeq 1.5b$. In general, the optimal junction size r does not vary significantly with B: from 26 Å for $B = 270\ k_BT$ Å^2 to 20 Å for $B = 450\ k_BT$ Å^2. As mentioned earlier, the relevant values of B are the lower ones ($B \approx 300\ k_BT$ Å^2) which correspond to long wormlike micelles. It should be noted however that ΔF decreases with B: from 22 to 14 k_BT as B increases from 270 to $B = 450\ k_BT$ Å^2. Yet, the physically more relevant free energy difference is $\Delta\tilde{F} = \Delta F - F_{ec}$, where F_{ec} is the end cap energy. $\Delta\tilde{F}$ is the free energy change in the end cap−cylinder fusion reaction mentioned above. The end cap energy, i.e, the packing free energy in a hemispherical cap relative to that in the cylinder, increases sharply as B decreases. Consequently $\Delta\tilde{F}$ increases with B. We shall return to this point after adding the chain contribution to ΔF. (Note that for $B = 300\ k_BT$ Å^2 we find $F_{ec} \simeq 22\ k_BT$, implying $\Delta\tilde{F} < 0$; see Figure 8).

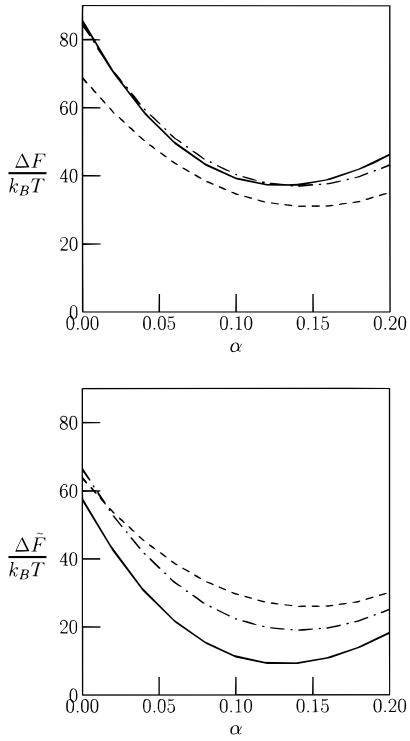

Figure 9. Junction energy ΔF (a, top) and fusion energy $\Delta\tilde{F}$ (b, bottom) (both minimized with respect to r) as a function of the relaxation parameter α, for different values of the head group interaction parameter: $B = 270\ k_BT$ Å^2 (solid line), $B = 330\ k_BT$ Å^2 (dashed−dotted line), and $B = 450\ k_BT$ Å^2 (dashed line).

Now we add the chain contribution to the packing energy in the junction, again optimizing ΔF with respect to r and then with respect to α. The results obtained for the variation of ΔF and $\Delta\tilde{F}$ with α (after minimization with respect to r) are shown in Figure 9, for several values of B. Again we see that ΔF decreases with B, but $\Delta\tilde{F}$ shows the opposite behavior. The optimal junction sizes are now somewhat larger than those obtained in the OFM approximation: $r \simeq 27$, 26, and 23 Å for B/k_BT Å^2 = 270, 330, and 450, respectively.

The calculations show that the head group and chain contributions to the junction energy are comparable. For instance; for $B = 270\ k_BT$ Å^2 we find $\Delta F = 38\ k_BT$ with 22 and 16 k_BT coming, respectively, from the head group and chain contributions to the free energy. The most significant result of our calculations is that, for the lowest (and most relevant) value of B for which cylinders are still more stable than bilayers, (namely, 270 k_BT Å^2 in our model), the free energy in the fusion reaction, though low, $\sim 10\ k_BT$, is positive. Thus, our calculations predict that in aqueous solutions of single surfactant component, which self-assembles into wormlike micelles, intermicellar junctions are energetically unfavorable but may appear as metastable structures.

5. Concluding Remarks

The calculations presented in this paper present the first attempt to estimate, on the basis of a molecular-level theory, the bending rigidity (hence the persistence length) of wormlike cylindrical micelles, as well as their propensity to form

intermicellar junctions. The calculations were limited to single-component surfactant solutions. The theory employed is approximate, as both the head group and the hydrocarbon chain contributions to the packing free energies were treated in a mean field level. Furthermore, our choice of molecular interaction parameters, though guided by experimental facts, is necessarily approximate. Nevertheless it should be remembered that approximate theoretical models of the kind used in the previous sections have been widely and successfully applied to calculate both single chain (conformational) and thermodynamic properties of self-assembled amphiphilic aggregates (for example, orientational bond order parameters of lipid chains in membranes and curvature elasticity moduli of monolayers and bilayers[27]).

For the persistence length of flexible, wormlike micelles we obtained values of just a few nanometers, in qualitative agreement with several experimental systems.[1] More precisely such low persistence lengths were observed in high-salt solutions of ionic surfactants where the electrostatic repulsion between the charged head groups is effectively screened. Qualitatively, in our model, this condition was mimicked by the small value of the parameter l_h. For stronger electrostatic repulsions a more detailed interaction model is called for.

The calculations pertaining to the formation of intermicellar junctions indicate that these structures are energetically metastable, at least when the optimal surface/volume ratio for amphiphile packing is intermediate between the cylindrical micelle and planar bilayer geometries. The existence of intermicellar junctions has been hypothesized on the basis of the unusual viscosity behavior observed in certain semidilute solutions of wormlike micelles.[5,6,19,20] Later on, intermicellar junctions were directly imaged by cryoelectron microscopy measurements,[25,26] yet it is not entirely clear whether these structures are (perhaps shear induced) metastable transients or equilibrium entities. Molecular dynamics simulations[23] of aqueous solutions of trimeric (three-tail) surfactant reveal some structures which appear as branched aggregates, yet the aggregates are rather globular and it is not clear that similar structures will be found in systems of truly long cylindrical micelles. Thus, presently, there is not sufficient evidence to either support nor refute our findings. Finally, we reiterate that the appearance of intermicellar junctions may be favored entropically, if not energetically. In a solution of overlapping wormlike micelles, junction formation (or transient "cross-linking") may provide an efficient alternative to entanglements and/or to high-energy end caps.[21,23]

Acknowledgment. We would like to thank Gregoire Porte, Mats Almgren, Jean Candau, Rony Granek, Ishi Talmon, Bill Gelbart, and Jacob Israelachvili for helpful discussions and comments. This work was supported by the US-Israel Binational Science Foundation and by the SFB 197, Germany. S.M. would like to thank the Minerva Stiftung for a postdoctoral fellowship. The Fritz Haber research center is supported by the Minerva Foundation, Munich.

Appendix

First we give a parametric description of the semitoroidal surface as shown in Figure 6. It can be defined by

$$x(\phi,\theta) = (\cos\phi)\{r + b\,[1 - \alpha(1 + \cos 6\phi)](\cos\theta)\}$$

$$y(\phi,\theta) = (\sin\phi)\{r + b\,[1 - \alpha(1 + \cos 6\phi)](\cos\theta)\} \quad (21)$$

$$z(\phi,\theta) = b\,[1 - \alpha(1 + \cos 6\phi)](\sin\theta)$$

with x, y, z being the Cartesian coordinates, $\pi/2 < \theta < 3\pi/2$ and $-\pi/6 < \phi < \pi/6$. According to this definition the torus thickness varies from $2b$ at $\phi = \pi/6$ to $2b(1 - 2\alpha)$ at $\phi = 0$. It is furthermore r, the torus radius measured with respect to the torus axis, and $0 \le \alpha$, a relaxation parameter, that give the pinching of the torus.

Using eqs 21 and the approximate treatment of the junction middle part as introduced in section 4, we can evaluate the overall junction area A and volume V which are in first order of α given by

$$A = b^2\left\{\left[2\chi^2\left(\sqrt{3} - \frac{\pi}{2}\right) + \pi(\pi\chi - 2)\right] - \pi\alpha(\pi\chi - 4)\right\}$$

$$V = b^3\left\{\left[2\chi^2\left(\sqrt{3} - \frac{\pi}{2}\right) + \frac{\pi}{6}(3\pi\chi - 4)\right] + \alpha[\pi(2 - \pi\chi) - \chi^2(13\sqrt{3} - 22)]\right\}$$

with $\chi = r/b$.

Evaluation of F in the semitoroidal sections of the junctions was carried out using eq 1, which can be written as

$$\frac{F}{3} = \int_{-\pi/6}^{+\pi/6} \mathrm{d}\phi \int_{\pi/2}^{3\pi/2} \mathrm{d}\theta\, \tilde{n} f(\phi,\theta) \quad (22)$$

with $\tilde{n}\,\mathrm{d}\phi\,\mathrm{d}\theta$ being the number of molecules in the angular element $\mathrm{d}\phi\,\mathrm{d}\theta$. It is in first order of α

$$\tilde{n} = \frac{b^2}{\nu}\left[\frac{1}{6}(3r + 2b\cos\theta) - 2\alpha\cos^2(3\phi)(r + b\cos\theta)\right]$$

In order to determine the head group contribution to F in eq 22, we need to know the area per molecule in the semitorus region, $a = \tilde{a}/\tilde{n}$. Here, $\tilde{a}\,\mathrm{d}\phi\,\mathrm{d}\theta$ is the area of the angular element $\mathrm{d}\phi\,\mathrm{d}\theta$. In first order of α one obtains

$$\tilde{a} = b[r + b\cos\theta - 2\alpha\cos^2(3\phi)(r + 2b\cos\theta)]$$

Finally, we note that the average bilayer thickness in the s region is given by

$$\tilde{l} = b\left[1 - \alpha\frac{12\sqrt{3} - 20}{12 - 3\sqrt{3} - 2\pi}\right] = b(1 - 1.507\alpha)$$

References and Notes

(1) Porte, G. In *Micelles, Membranes, Microemulsions and Monolayers*; Gelbart, W. M.; Ben-Shaul, A.; Roux, D., Eds.; Springer: Berlin, 1994; Chapter 2.
(2) Vinson, P. K.; Talmon,Y. *Science* **1990**, *133*, 288.
(3) Edwards, K.; Almgren, N. *J. Colloid Interface Sci.* **1991**, *147*, 1.
(4) Cates, M. E.; Candau, S. J. *J. Phys.: Condens. Matter* **1990**, *2*, 6869.
(5) Candau, S. J.; Khatory, A.; Lequeux, F.; Kern, F. *J. Phys IV* **1993**, *3*, 197.
(6) Candau, S. J.; Hirsch, E.; Zana, R. *J. Colloid Interface Sci.* **1985**, *105*, 521.
(7) Rehage, H.; Hoffmann, H. *J. Phys.Chem.* **1988**, *92*, 4712.
(8) Israelachvili, J. N. *Intermolecular and Surface Forces*, 2nd ed.; Academic Press: New York, 1992.
(9) Israelachvili, J. N.; Mitchell, D. J.; Ninham, B. W. *J. Chem. Soc., Faraday Trans. 1* **1976**, *72*, 1525.
(10) Tanford, C. *The Hydrophobic Effect*, 2nd ed.; Wiley: New York, 1980.
(11) Ben-Shaul, A.; Gelbart, W. M. In *Micelles, Membranes, Microemulsions and Monolayers*; Gelbart, W. M., Ben-Shaul, A., Roux, D., Eds.; Springer: Berlin, 1994; Chapter 1.
(12) Gelbart, W. M.; Ben-Shaul, A. *J. Phys. Chem.* **1996**, *100*, 13169, and references cited therein.
(13) Grosberg, A. Y.; Khokhlov, A. R. *Statistical Physics of Macromolecules*; AIP Press: New York, 1994.
(14) de Gennes, P. G. *Scaling Concepts in Polymer Physics*; Cornell University Press: Ithaka, NY, 1979.
(15) Odijk, T. *J. Phys. (Paris)* **1987**, *48*, 125. Odijk, T. *Macromolecules* **1986**, *19*, 2313. Duyndam, A.; Odijk, T. *Langmuir* **1996**, *12*, 4718.

(16) Hentschke, R. *Liq. Cryst.* **1991**, *10*, 691.
(17) Mc Mullen, W. E.; Gelbart, W. M.; Ben-Shaul, A. *J. Chem. Phys.* **1985**, *82*, 5616.
(18) van der Schoot, P.; Cates, M. E. *Europhys. Lett.* **1994**, *25*, 515. van der Schoot, P. *J. Chem. Phys.* **1996**, *104*, 1130. van der Schoot, P. *Macromolecules* **1994**, *27*, 6473.
(19) Appel, J.; Porte, G.; Khatory, A.; Kern, F.; Candau, S. J. *J. Phys.* **1992**, *2*, 1045.
(20) Khatory, A.; Lequeux, F.; Kern, F.; Candau, S. J. *Langmuir* **1993**, *9*, 1456. Khatory, A.; Kern, F.; Lequeux, F.; Appell, J.; Porte, G.; Morie, N.; Ott, A.; Urbach, W. *Langmuir* **1993**, *9*, 933.
(21) Drye, T. J.; Cates, M. E. *J. Chem.Phys.* **1982**, *96*, 1367.
(22) Elleuch, K.; Lequeux, F.; Pfeuty, P. *J. Phys. I* **1995**, *5*, 465.
(23) Bohbot, Y.; Ben-Shaul, A.; Granek, R.; Gelbart, W. M. *J. Chem.Phys.* **1995**, *103*, 8764.
(24) Karaborni, S.; Esselink, K.; Hilbers, P. A. J.; Smit, B.; Karthauser, J.; van Os, N. M.; Zana, R. *Science* **1994**, *266*, 254.
(25) Gustafsson, J.; Oradd, G.; Lindblom, G.; Olson, U.; Almgren, M. *Langmuir* **1997**, *13*, 852.
(26) Danino, D.; Talmon, Y.; Levy, H.; Beinert, G.; Zana, R. *Science* **1995**, *269*, 1420.
(27) For a review see e.g.: Ben-Shaul, A. In *Structure and Dynamics of Membranes*; Lipowsky, R., Sackmann, E., Eds.; Elsevier: Amsterdam, 1995; Chapter 7.
(28) Szleifer, I.; Kramer, D.; Ben-Shaul, A.; Gelbart, W. M.; Safran, S. A. *J. Chem. Phys.* **1990**, *92*, 6800.
(29) May, S.; Ben-Shaul, A. *J. Chem. Phys.* **1995**, *103*, 3839.
(30) Porte, G.; Gomati, R.; El Haitamy, O.; Appel, J.; Marignan, J. *J. Phys. Chem.* **1986**, *90*, 5746.
(31) Helfrich, W. *Z. Naturforsch.* **1973**, *28c*, 693.